

# Calculations of Low-Mach-Number Viscous Flows without Preconditioning by the Space-Time CE/SE Method

Zeng-Chan Zhang<sup>1</sup>, S.T. John Yu<sup>1</sup>, Sin-Chung Chang<sup>2</sup>, and Philip C.E. Jorgenson<sup>2</sup>

<sup>1</sup>Mechanical Engineering Department, Wayne State University, Detroit, MI 48202, USA

<sup>2</sup>NASA Glenn Research Center, Cleveland, OH 44135, USA

**Abstract.** In this paper, we report the calculations of low-Mach-number viscous flows without preconditioning by the space-time CE/SE method [12,3]. It is shown that the CE/SE method can sustain highly resolved solution for long-term calculations with large numbers of time steps. Several numerical examples are calculated to demonstrate the efficiency and accuracy of the CE/SE method in calculating low-speed flows.

## 1. Introduction

Many low-Mach-number flows contain both compressibility effects and low-speed regions, and the compressible equations must be used in the model. For example, low speed flows with significant temperature variations are compressible due to density variation induced by heat addition. Although flow speeds are slow, one must employ the compressible flow equations to model these flow fields. However, it is well known that the conventional CFD methods, which can handle high-speed compressible flow easily, fail miserably when applied to low-Mach-number flows. In the past, due to wide applications of low-speed compressible flows, extensive studies have been conducted to construct viable numerical methods [4,5]. Conventional approaches can be divided into two categories: the pressure-based methods and the density-based methods. The pressure-based methods are extension of the projection method for incompressible flows. The SIMPLE schemes are typical examples. The density-based methods are extension of methods for compressible flows with two modifications: (1) adding a pseudo compressibility term to the continuity equation, and (2) preconditioning the Jacobian matrix of the convection terms such that the eigenvalues are artificially brought closer to each other. Combination of the two special treatments enables one to fabricate an artificial hyperbolic system, which is amenable to be solved by conventional CFD methods in a limited number of time steps.

To date, the newly developed space-time CE/SE method [1,2,3] has been used to calculate high-speed flows with shocks and aero acoustic flows. In this paper, we apply the CE/SE method to low-Mach-number compressible flows as well as incompressible by using the same flow solver for high speed flows. We show that numerical difficulties encountered when using the conventional CFD methods to calculate low-Mach-number flows do not exist if the space-time CE/SE method was used. Demonstrated by numerical examples, we show that the same CFD code, which has been used for shock capturing in high-speed flows, can be directly applied to low-Mach-number flows without any modification. We

remark that the size of the time step employed in the present calculations is still restricted by the CFL number and the von Neumann number. Thus a large number of time steps are needed to march the flow solution to its full development. Note that when conventional methods without preconditioning were used, false solutions would be obtained due to excessive artificial damping and accumulation of errors. The preconditioning procedure will artificially enhance numerical wave propagation and thus reduce the number of time steps required for calculations. As such, the error accumulation by the numerical schemes is avoided. Therefore, the key issue here is *whether the numerical scheme employed can sustain highly accurate solution for a large number of time steps*. This issue is not restricted to low-speed flows only. In simulating a propagating normal shock over a long period of time, all upwind schemes show the so-called carbuncle effect, leading to numerical overflow.

The surprising finding reported here shows that the CE/SE method maintains the integrity of the flow solution when the simulation is carried out in a large number of time steps. In other words, the accumulation of errors is minimum, and the local and global flux conservation in a space-time sense has been truly maintained. In this paper, we first briefly summarize the CE/SE method for Navier Stokes equation. Then three numerical examples are included to demonstrate capabilities of the newly developed Navier-Stokes solver for solving these low-speed flows.

## 2. The CE/SE Method for the Navier Stokes Equations

Consider the following two-dimensional Navier-Stokes Equations,

$$\frac{\partial U_m}{\partial t} + \frac{\partial f_{im}}{\partial x} + \frac{\partial g_{im}}{\partial y} - \frac{\partial f_{vm}}{\partial x} - \frac{\partial g_{vm}}{\partial y} = 0, \quad (2.1)$$

where  $m = 1, 2, 3, 4$  for the continuity,  $x$  and  $y$  momentum and the energy equations, and  $U = (\rho, \rho u, \rho v, E_v)$ . Here  $f_{im}$  and  $g_{im}$  are the inviscid fluxes, and  $f_{vm}$  and  $g_{vm}$  are viscous ones. Let  $x_1 = x$ ,  $x_2 = y$  and  $x_3 = t$  be the coordinates of a three-dimensional Euclidean space  $E_3$ . The integral counterpart of Eq. (2.1) is

$$\oint_{S(V)} \vec{h}_m \cdot d\vec{s} = 0, \quad m = 1, 2, 3, 4 \quad (2.2)$$

Here  $S(V)$  is the boundary surface of a space-time region  $V$  in  $E_3$ , and  $\vec{h}_m = (f_{im} - f_{vm}, g_{im} - g_{vm}, U_m)$ , and it can be decomposed into the following inviscid and viscous parts:

$$\vec{h}_m = \vec{h}_{im} - \vec{h}_{vm} = (f_{im}, g_{im}, U_m) - (f_{vm}, g_{vm}, 0) \quad (2.3)$$

To perform the space-time integration in two spatial dimensions, triangular spatial mesh is used. Refer to Fig. 1. The grid points are distributed at the center of each triangle. In connection with its three neighbors, we define three conservation elements (CEs) and one solution element (SE) associated with each mesh node. At point G, three CE<sup>(l)</sup> ( $l=1,2,3$ ) are the cylinders ABGFA'B'G'F', BCDGB'C'D'G' and DEF GD'E'F'G'. The SE is the union of four planes ABCDEF, G'G''F'F', G'G''B''B', G'G''D''D' and their immediate neighborhood.

Inside each  $SE(j, n)$ , the flow variables are assumed continuous, and the first-order Taylor series expansions is used to approximate  $U_m(x, y, t)$ ,  $f_{im}(x, y, t)$  and  $g_{im}(x, y, t)$ . To calculate the viscous fluxes, the midpoint rule is used. From Eq. (2.3), the third component of  $h_{vm}$  is a null. Thus, in calculating the viscous fluxes, we only need to calculate integrals over lateral surfaces in the space-time domain. For example, in  $CE^{(2)}$ , the quadrilateral cylinder  $ABGFA'B'G'F'$ , we only need to integrate the viscous terms over four lateral surfaces  $ABA'B'$ ,  $AFA'F'$ ,  $GBG'B'$  and  $GF'G'F'$ . Consider the integral of  $h_{vm}$  on the surface  $AFA'F'$ , using the midpoint rule:

$$\int_{AFA'F'} h_{vm} \cdot d\vec{S} \approx S_x \cdot f_{vm}((U_m, U_{mx}, U_{my})_Q^{n-1/4})_{n-1/2} + S_y \cdot g_{vm}((U_m, U_{mx}, U_{my})_Q^{n-1/4}) \quad (2.4)$$

where  $\Delta \vec{S} = (S_x, S_y, S_t)$  is the surface vector, defined as the unit outward normal vector multiplied by its area. And  $Q$  is the centroid of surface  $AFA'F'$ . Because the surface  $AFA'F'$  belong to the  $SE$  of point  $A'$ , we can use the parameters at point  $A'$  to approximate  $U_m$ ,  $U_{mx}$  and  $U_{my}$  at point  $Q$ . Similar procedure is performed for surfaces  $ABA'B'$ ,  $GBG'B'$  and  $GF'G'F'$ .

The space-time flux conservation over the three  $CE$ 's provides three algebraic equations for the three unknowns,  $U$ ,  $U_x$  and  $U_y$  at each mesh node. Since the viscous terms are included, the addition of the artificial damping as that in the  $a-\varepsilon$  scheme is optional. For flow with shocks, a re-weighting procedure is used for the jump condition, i.e., the  $a-\alpha$  scheme [1,2]. This concludes the brief description the  $CE/SE$  method for solving the two-dimensional Navier-Stokes equations.

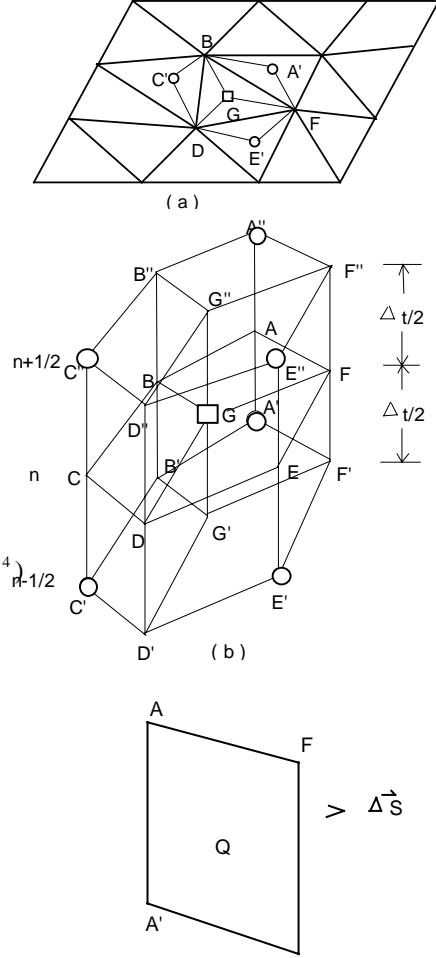


Fig. 1 A schematic of the  $CE/SE$  scheme: (a) triangle mesh in two spatial dimensions; (b) The definitions of the  $CE$ 's and  $SE$ ; (c) the calculation of the space-time flux.

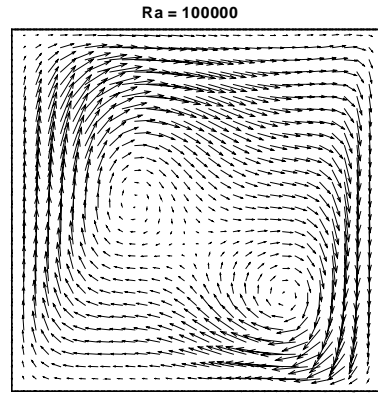
### 3. Numerical Results

Three low-Mach-number flows are calculated using the viscous CE/SE scheme. On the wall boundaries, a newly developed unified solid boundary treatment [6] is used. On the outlet and/or open boundaries, the non-reflective boundary condition is used.

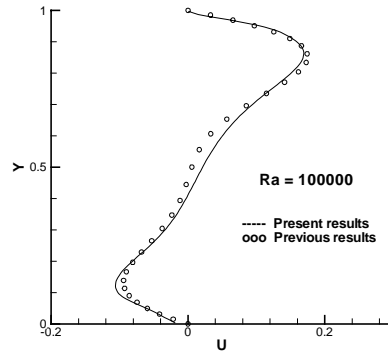
#### 3.1 Buoyancy-driven gas flows

The first example is a buoyancy-driven gas flow in a square box. The configuration consists of two insulated horizontal walls and two lateral walls with constant temperatures of  $T_h$  (left) and  $T_c$  (right). For a small temperature difference between these two vertical walls, this problem has been extensively studied based on the incompressible flow equations with Boussinesq model for buoyancy force. For a large temperature difference, the compressible formulation must be employed.

The flow features of this buoyancy-driven cavity flow depend on Rayleigh number  $R_a$ , Froude number  $F_r$ , the aspect ratio of the cavity, and the temperature difference parameter  $\epsilon$ . Here only one case is shown in Fig.2 with Rayleigh number  $R_a = 10^5$  and temperature difference parameter  $\epsilon = 0.6$ , which represents  $T_h/T_c = 4$ . The Froude number and the aspect ratio are unity. 7200 triangles (cells) are used. The calculation reaches the steady-state solution after about 10,000 iterations. Fig.2 shows the velocity vectors and x-direction velocity distribution along the vertical centerline. The solution agrees well with previously reported data [7].



(a)



(b)

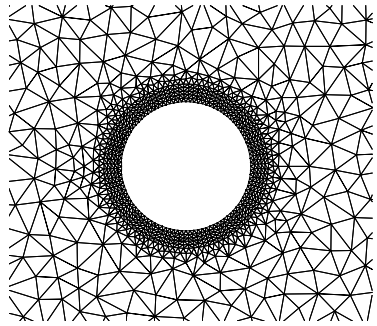
Fig.2 Solution of the buoyancy-driven flow, (a) Velocity vectors, (b)  $u$  along the vertical centerline.

#### 3.2 Driven Cavity Flow

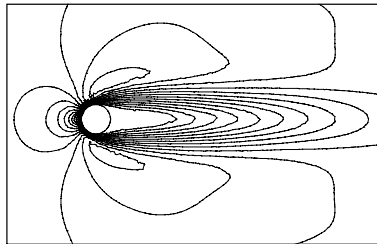
This is a benchmark problem for incompressible viscous flow calculations. Here the full compressible Navier-Stokes equations are solved to demonstrate the capabilities of the CE/SE scheme at the incompressible limit. 7,688 triangles are used. Figure 3 shows velocity vectors, and x-velocity distribution along the vertical centerline at  $Re = 1000$ . This solution agrees well with Ghia's data [8].

### 3.3 Flows over a circular cylinder

The third example is an external flow over a circular cylinder. First, we consider  $Re = 40$ , and a steady-state solution is shown in Fig. 4. Again, the full compressible equations are solved by the CE/SE method without preconditioning. The computational domain is  $[-5, 15] \times [-5, 5]$ , and 10,092 triangles are used. Figure 4(a) shows the unstructured mesh near the circular cylinder. Figures 4(b)-(c) show the velocity vectors and Mach number contours of the flow solution. The location of the boundary layer separation on the cylinder surface and the size of the recirculating region ( $L/d \approx 2.0$ ) compare favorably with the experiment data [9]. If the Reynolds number is increased to 200, the flow becomes unsteady, and Fig. 5 shows vorticity contours at two different times. The oscillating frequency compares well with the experimental data.



(a)



(c)

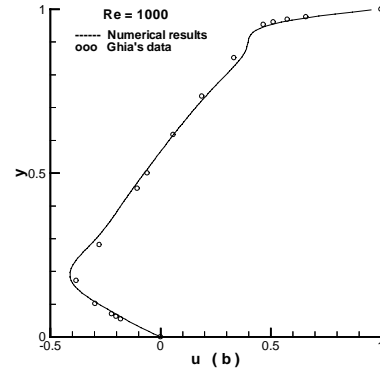
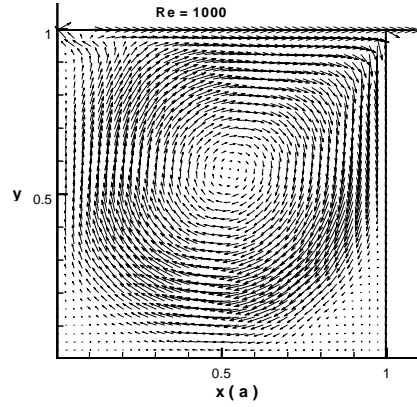
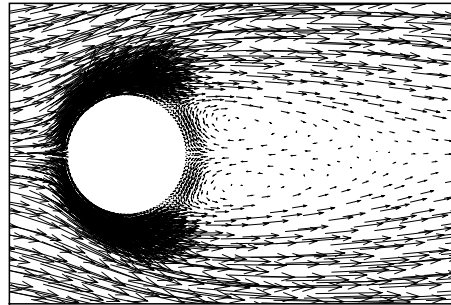


Fig.3. Solution of a driven cavity flows: (a) Velocity vectors and (b)  $u$  along the vertical centerline.



(b)

Fig.4. A flow over a cylinder ( $Re = 40$ ): (a) Mesh around the cylinder, (b) velocity vectors, and (c) Mach number contours.

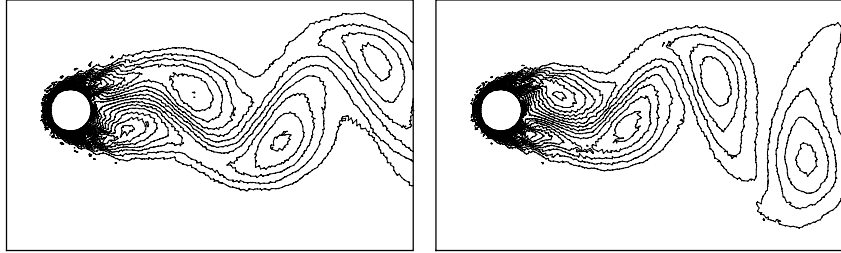


Fig.5. Vorticity contours of the flow over a cylinder ( $R_e = 200$ ) at two different time steps.

#### 4. Concluding Remarks

In this paper, we report the applications of the CE/SE method to low-speed flows without preconditioning. Numerical results show that the present CE/SE method for Navier Stokes equations can be used for flows at all speeds without preconditioning. This surprising finding, mainly achieved by low numerical dissipation in calculating space-time flux conservation, is in contrast to the traditional wisdom of treating low-Mach number flows. It shows that the present CE/SE solver can maintain solution integrity for calculation with a large number of time steps and error accumulation has been avoided by space-time flux conservation and a robust non-reflective boundary condition.

#### References

1. Chang, S.C., *J. Comp. Phys.*, **119**, pp. 295-324, 1995.
2. Chang, S.C., Wang, X.Y. and Chow, C.Y., *J. Comp. Phys.*, **156**, pp.89-136, 1999.
3. Zhang, Z.C., Yu, S.T., Chang, S.C., Himansu, A. and Jorgenson, P., AIAA Paper 99-3277, June. 1999.
4. Choi, D. and Merkle, C.L., *AIAA J.*, **23**, p.1518, 1985.
5. Choi, Y.H., Ph.D. Thesis, The Pennsylvania State University, 1989.
6. Chang, S.C., Zhang, Z.C., Yu, S.T. and Jorgenson, P., Proceeding of ICCFD, Kyoto, Japan 2000.
7. Yu, S.T., Jian, B.N., Wu, J. and Liu, N.S., *Comput. Methods Appl. Mech. Engrg.*, **137**, pp. 59-88, 1996.
8. Guia, U., Guia, K.N. and Shin, C.T., *J. Comp. Phys.*, **48**, pp. 387-411, 1982.
9. Dennis, S.C.R. and Chang, G.Z., *J. Fluid Mechs.*, **42**, 471-489, 1970.